

Critical current density of coated conductors determined from rescaled magnetic moment at temperatures close to 77 K



E. Seiler^{*,a}, F. Gömöry^a, J. Mišík^b, D. Richter^c

^a Institute of Electrical Engineering, Slovak Academy of Sciences, Dúbravská cesta 9, Bratislava, 841 04 Slovakia

^b Faculty of Materials Science and Technology in Trnava, Slovak University of Technology, Jána Bottu 25, Trnava 917 24 Slovakia

^c CERN, CH-1211 Geneva 23, Switzerland

ARTICLE INFO

Keywords:

Coated conductors
Critical current density
Magnetic measurements

ABSTRACT

The possibility of rescaling (or calibrating) of the magnetization results to predict the transport critical current density (J_c) of commercial coated conductors (REBCO tapes) is discussed from both the experimental and theoretical point of view. For this purpose the critical current density in tapes from three different producers was investigated by means of transport and magnetization measurements, in perpendicular magnetic fields of 0.25 T – 2 T at temperatures 65 K – 77 K. Two kinds of samples were tested in the magnetization measurements – square samples $2 \times 2 \text{ mm}^2$ cut from the central parts of the tapes and elongated rectangular samples of the full tape width (4 mm nominally) and 8 mm length. The transport measurements were performed on full-width samples in a subcooled liquid nitrogen bath. The presented results show that it is possible to empirically rescale the measured magnetization data on the basis of a single transport measurement, achieving the overall accuracy of the transport J_c prediction between 4% and 10% for different tested tapes. Simple theoretical justification and analysis of the empirical scaling is presented, based on the critical state model with the power law current-voltage relation considered to account for different level of electric field in the transport and magnetization measurements.

1. Introduction

Technical high temperature superconducting wires of the 2nd generation, the Coated Conductors (CC's) [1–3], are being studied and tested for applications in a wide range of working temperatures [4–7]. One of very perspective areas are the rotating electric machines, involving temperatures below the boiling point of liquid nitrogen 77 K and magnetic fields up to a few Tesla [8–13]. Our study was focused on this domain of temperatures and magnetic fields. With continuing improvement of the current carrying capabilities of the CC's the level of transport currents necessary for I_c determination can be expected to further rise in the future [14]. Then, a reliable determination of the critical current I_c in standard transport measurements can be at lower temperatures complicated due to the heat generation, either in the sample itself, at the current contacts or in the current leads.

The difficulties connected with the heat generation are often at least partially overcome by physically narrowing the CC original width, thus reducing the required transport current, or by employing pulsed transport current measurement methods [15–18]. Another alternative represent the contactless magnetization measurements where sample heating is avoided, offering thus in general much broader interval of

available magnetic fields and temperatures than the transport ones. However, determination of critical current from these measurements is indirect, based on the relation between the critical current density J_c and the sample's magnetic moment m . Calculation of J_c from the magnetic moment involves some simplifying assumptions regarding the sample geometry and the current distribution, which can lead to a deviation of the J_c determined in the magnetization measurement from its value measured directly in transport experiment.

Nonetheless, previous studies [19] indicate that a simple recalculation, or empirical scaling, of the magnetization-determined J_c to match the transport one works satisfactorily for coated conductors at lower temperatures (5 K – 40 K) and higher applied magnetic fields (3 T – 9 T). The goal of the presented work was to explore the possibility of substituting the transport critical current measurements with the magnetization ones for commercially available CC's at higher temperatures and lower fields. In order to obtain an extensive set of experimental data determined by both techniques we have focused on the temperature interval 65 K – 77 K where we were able to perform both the standard transport I_c measurements in a subcooled liquid nitrogen bath as well as the magnetization measurements. As expected, quantitative analysis revealed some differences between transport and

* Corresponding author.

E-mail address: eugen.seiler@savba.sk (E. Seiler).

Table 1

Basic parameters of the investigated REBCO tapes, dimensions of the square-shaped and rectangular magnetization samples and the scaling factors discussed in Sections 3 and 4. (t – thickness of superconducting layer, w – width and l – length of the sample).

	Superox	Sunam	Superpower
Technol.:	PLD	RCE *	MOCVD
† J_c [A]	154	247	112
t [μm]	1.306	1.506	1.819
Square:			
w	1.94 mm	1.96 mm	1.97 mm
l	1.98 mm	2.03 mm	2.00 mm
emp. F_{77}	$3.25 \cdot 10^{14} \text{ m}^{-4}$	$3.18 \cdot 10^{14} \text{ m}^{-4}$	$2.42 \cdot 10^{14} \text{ m}^{-4}$
theo. ϕ_{77}	$3.67 \cdot 10^{14} \text{ m}^{-4}$	$2.87 \cdot 10^{14} \text{ m}^{-4}$	$2.69 \cdot 10^{14} \text{ m}^{-4}$
Rectang.:			
(full sc) w	3.90 mm	3.91 mm	3.84 mm
l	7.90 mm	8.84 mm	8.80 mm
emp. F_{70}	$1.96 \cdot 10^{13} \text{ m}^{-4}$	$1.22 \cdot 10^{13} \text{ m}^{-4}$	$1.18 \cdot 10^{13} \text{ m}^{-4}$
theo. ϕ_{70}	$1.71 \cdot 10^{13} \text{ m}^{-4}$	$1.26 \cdot 10^{13} \text{ m}^{-4}$	$1.15 \cdot 10^{13} \text{ m}^{-4}$

*Reactive Co-Evaporation; †77 K, self-field; ‘emp.’ = empirical; ‘theo.’ = theoretical.

magnetization-based J_c values. The most important aspects are discussed in this paper, with the aim to test whether, and to which extent, could a scaling factor determined at one temperature be possibly used in a broader temperature interval.

2. Experimental details

Commercial coated conductors, called also REBCO tapes, of 4 mm nominal width from three manufacturers were investigated in the study: SCS4050-AP wire from Superpower Inc. (denoted as ‘SP’ further), HCN 04150 tape from SuNAM Co., Ltd. (‘Sunam’) and the REBCO tape produced by SuperOx company (‘Superox’) [20–22]. Some of the basic characteristics of the tapes are summarized in the Table 1.

In the transport measurements, the current-voltage curves (I-V curves) were measured at constant temperature employing standard four point method in a constant homogeneous magnetic field applied perpendicular to the wide face of coated conductor. Measurements were performed on samples of full CC width (~ 4 mm). Current leads were soldered at the extremities of the approximately 8 cm long samples, the pairs of voltage sensing wires – voltage taps – were soldered in the central part of the samples with typically 1 cm distance between the taps. The critical current I_c was determined from the measured I-V curves using the common $1\mu\text{V}/\text{cm}$ voltage criterion.

The sample was attached to a supporting fiberglass plate and immersed in a liquid nitrogen bath inside a non-metallic, vacuum tight cryostat. The liquid nitrogen bath was subcooled below 77 K by pumping the nitrogen vapour out of the cryostat and stabilizing reduced vapour pressure at the necessary level. The transport I-V measurements in subcooled liquid nitrogen bath were performed at temperatures $T = 65$ K, 67 K, 70 K, 73 K and 77 K (bath at atmospheric pressure). Temperature of the sample was monitored during the transport measurements with a Cernox thermometer (CX-1050-SD) attached to the central part of the sample between the voltage taps. Temperature variations during the I-V measurement were typically at the level of 0.05 K, but always less than 0.15 K. For each sample at each temperature a series of I-V measurements in applied magnetic field $B = 0.25, 0.5, 0.75, 1, 1.25, 1.5, 1.75, 2$ Tesla was performed. The effects of the self-field generated by the transport current can be neglected at these magnitudes of the applied magnetic field.

The magnetization measurements were performed using a Vibrating Sample Magnetometer (VSM). Magnetic moment m was measured at constant temperature T while continuously sweeping the external homogeneous magnetic field B applied perpendicular to the wide face of the tape. Constant sweep rate s was employed in all the

measurements and the magnetization loops were recorded when changing the applied field between extremal values of $B = -3$ T and $B = +14$ T (i.e. following $B = 0 \rightarrow -3$ T $\rightarrow +14$ T $\rightarrow -3$ T). This sequence guaranteed the full saturation of the REBCO superconducting layer by the critical current density. The parts of the magnetization loops between 0 and 14 T were used to determine the width of the magnetization loop Δm , equal to $2 \times$ the irreversible magnetic moment that is proportional to the critical current density. Measurement temperatures were the same as in the transport measurements (65, 67, 70, 73, 77 Kelvin). The basic set of magnetization measurements was performed using the sweep rate $s = 6.3$ mT/s = 0.378 T/min, another two sets of measurements were performed at $s = 3$ mT/s and $s = 12$ mT/s to test the effect of the sweep rate on the results. No influence of the weakly magnetic Hastelloy substrate on the irreversible part of the magnetic moment has been observed. All reversible (non-hysteretic) contributions were eliminated in the standard determination of the magnetization loop width as the difference between the magnetic moment at a given applied field B in the positive branch of the loop, $m^+(B) > 0$, and the magnetic moment in the negative branch, $m^-(B) < 0$, so that $\Delta m(B) = m^+(B) - m^-(B)$.

Samples of practically square shape, approximately 2×2 mm², were cut from the middle part of the investigated REBCO tapes for magnetization measurements in the VSM set-up at IEE Bratislava. An oscillating wire saw was used to cut the samples, the resulting cut edges were very clean and smooth. No damage of the edges was observed in an optical microscope and in a scanning electron microscope (SEM), in particular no signs of delamination were detected in case of all three tapes. SEM images of the edge areas of the samples are shown in the Fig. 1 for illustration.

For comparison, one set of measurements was performed in a VSM set-up at CERN Geneva, at the temperature $T = 70$ K and sweep rate $s = 6.3$ mT/s. Thanks to significantly bigger sample space in the CERN VSM, rectangular samples of the full tape width (4 mm nominally) and with the length of approximately 8 mm were used in these measurements. Regarding the geometrical dimensions of the samples in the Table 1, the thickness t and the full width of the superconducting layer (‘full sc’) were determined from the SEM micrographs, the other dimensions were determined in an optical microscope.

3. Empirical comparison of results

Direct comparison of the experimental transport $J_c(B)$ and magnetization $\Delta m(B)$ dependences at all temperatures shows that the

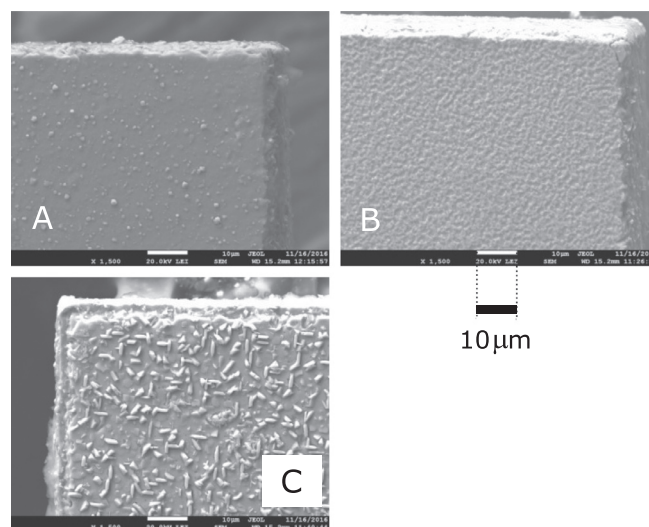


Fig. 1. SEM images of edges of the square-shaped samples cut from the REBCO tapes. The stabilizing Cu layer was etched off and the REBCO layer is visible at the surface of the samples. A – Superox, B – Sunam, C – Superpower.

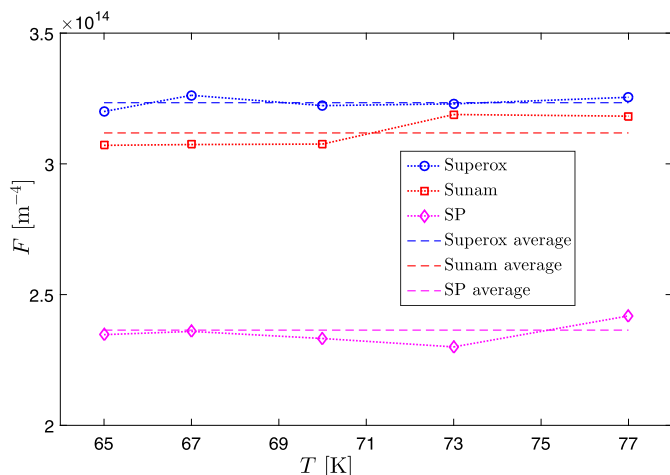


Fig. 2. Empirical scaling factors F in dependence on temperature.

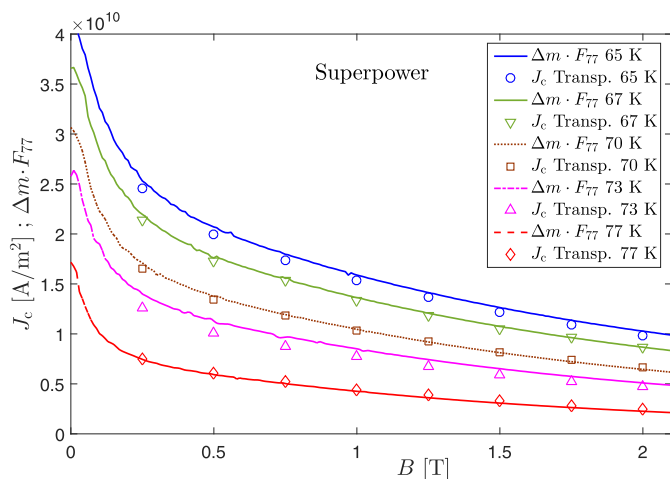


Fig. 3. Critical current density determined in transport measurement, $J_c(B)$, compared with the data from magnetization loops, $\Delta m(B)$, scaled with the same numerical factor F_{77} for all temperatures. Sample $2 \times 2 \text{ mm}^2$ cut from the Superpower tape, $s = 6.3 \text{ mT/s}$.

transport values can be obtained from the magnetization data with the help of an empirical scaling factor $F(T)$:

$$J_c(B, T) = F(T) \Delta m(B, T). \quad (1)$$

Although the scaling factor F does depend on temperature, in the explored temperature range this dependence is only very moderate as illustrated in Fig. 2. It could be calculated at any B at which both the Δm and J_c experimental values are available, in our case we chose $B = 0.25 \text{ T}$ thus $F(T) = J_c(0.25 \text{ T}, T) / \Delta m(0.25 \text{ T}, T)$.

Due to the moderate temperature dependence, it is in practice possible to use a single value of F to scale the $\Delta m(B)$ dependences at all temperatures, achieving still a very reasonable accordance with the transport $J_c(B)$. This value can be determined on the basis of a single transport measurement performed at experimentally convenient conditions, for example at $T = 77 \text{ K}$ and $B = 0.25 \text{ T}$. Using the $F(77 \text{ K})$, referred further as F_{77} for simplicity, to scale the measured magnetization curves yields in the case of Superox and Superpower tapes the maximum relative difference with respect to the transport J_c of approximately 4%, only at a few highest fields at 77 K up to 10%. In the case of the Sunam tape the typical relative difference is up to $\sim 10\%$, reaching up to 25% at the highest fields at 77 K. The somewhat less accurate agreement observed for Sunam tape is from the most part connected with the decrease of the I-V curve n -exponent (see (3)) with

temperature and field, as is discussed in following sections. Variation of the n -exponent for Sunam tape is the biggest among all the three tapes and the variation has in general the biggest impact at the highest applied fields.

Fig. 3 shows a comparison of the transport $J_c(B)$ dependences with the magnetization $\Delta m(B)$ for the Superpower tape, where the factor F_{77} was used to rescale the $\Delta m(B)$ at all temperatures. Similarly high degree of accordance is observed also in the case of the Superox and Sunam coated conductors. From the experimental point of view it thus seems feasible to scale, or “calibrate”, the measured $\Delta m(B)$ curves on the basis of a single transport measurement.

An important point to note is that the applied magnetic field should be high enough to be able to neglect the transport current self-field effects and to ensure full sample penetration with single direction screening currents in the corresponding magnetization measurement.

4. Theoretical relation between transport and magnetization results

4.1. Basic considerations

From theoretical point of view, in the framework of the critical state model [23] the magnetic moment of superconducting sample Δm in fully saturated state is directly proportional to its critical current density J_c through a geometrical constant C_g , which depends only on the geometry of the screening currents flowing in the sample. However, the real $E(J)$ relation – the relation between the current and electric field E in the superconductor – is smooth and therefore the value of the electric field at which the transport I_c and the Δm are determined should be considered as well [24,25].

Several theoretical models exist for superconductors of idealized geometrical shapes [26–29] that describe the magnetic flux penetration into the superconducting volume, yielding simple algebraic expressions for the geometrical constant C_g . However, considering a general, rectangular-prism-shaped superconductor of any thickness in the fully penetrated state, the saturated magnetic moment m_{sat} is expressed with a simple relation [30–32]:

$$|m_{\text{sat}}| = \Delta m / 2 = \frac{1}{4} j t w^2 l \left(1 - \frac{w}{3l} \right), \quad (2)$$

where j is the (critical) density of circulating currents, w and l are the dimensions of the cross section in the plane perpendicular to the applied magnetic field ($w \leq l$) and t is the dimension parallel to the applied field. In our case the t , w , l are, respectively, the thickness, width and length of the thin, prism-shaped superconducting layer of the REBCO tape placed in magnetic field applied parallel to the thickness t .

On the other hand, the increase of electric field in the superconductor in the region of the transition into the dissipative state with unpinned vortex lattice is in most cases very well described by the widely used power law function:

$$E = E_c \left(\frac{J}{J_c} \right)^n. \quad (3)$$

The E_c here represents the electric field at which the critical current density J_c is determined, so-called electric field criterion. The $E(J)$ dependence was measured in the transport experiments and the critical current (current density) was determined at the commonly used $E_c = 1 \mu\text{V/cm}$ – denoted as the transport critical current density J_c .

However, the level of electric field in the superconducting sample during the magnetization measurements is in most cases different from the E_c employed to determine the transport critical current. Typically it is smaller, often by one or two orders of magnitude. In order to estimate the level of electric field in a simple way we considered the electric field induced at the circumference of the sample as a typical electric field, although it does actually represent the maximal electric field in the

sample. Considering a sample with rectangular cross section $w \times l$ in the plane perpendicular to the applied magnetic field, which is being swept with a constant sweep rate $s = dB/dt$, the magnitude of the electric field $E_{i,\text{mag}}$ induced at the circumference is given by a simple expression:

$$E_{i,\text{mag}} = lws/(2l + 2w). \quad (4)$$

The density of currents circulating in the sample in the magnetization measurements j corresponds to this electric field, so that $j = J(E_{i,\text{mag}})$.

Further we assumed that the same power law function (3) can be used to describe the $E(J)$ relation also at electric fields considerably lower than E_c , using the same exponent n determined in the transport measurements. Although n does in fact depend also on the electric field, in our case, when the typical value of $E_{i,\text{mag}}$ is $\sim 0.03 \mu\text{V}/\text{cm}$, the change in n with respect to the value determined around $1 \mu\text{V}/\text{cm}$ is not expected to be very significant [24], most probably at the level $\Delta n \approx 1$ to 2. Then it follows from (3) and (4):

$$j = \left(\frac{E_{i,\text{mag}}}{E_c} \right)^{1/n} J_c = \left(\frac{lws}{2(l+w)E_c} \right)^{1/n} J_c \equiv K_e J_c, \quad (5)$$

where K_e is introduced as an electric field correction factor. Combining (5) and (2) one arrives to a theoretical relation connecting the experimental transport J_c and experimental Δm values:

$$J_c K_e = \Delta m \left[t w^2 l \left(1 - \frac{w}{3l} \right) / 2 \right]^{-1} \equiv \Delta m C_g. \quad (6)$$

4.2. Empirical and theoretical scaling factor

From the considerations above it follows that theoretical recalculation of the magnetic moment to the transport critical current density is determined by two factors – the geometrical constant C_g and the electric field correction K_e :

$$C_g = 2 \left[t w^2 l \left(1 - \frac{w}{3l} \right) \right]^{-1}; \quad K_e = \left(\frac{lws}{2(l+w)E_c} \right)^{1/n(B,T)}. \quad (7)$$

Based on (1) and (6) one can easily identify the theoretical counterpart φ of the empirical scaling factor:

$$F \leftrightarrow \varphi = C_g / K_e. \quad (8)$$

The geometrical constant C_g is determined solely by the geometrical dimensions of the sample used in magnetization experiments. On the other hand, the electric field correction K_e involves apart from the geometrical dimensions also the experimental parameters E_c and s and particularly the power law exponent $n(B, T)$, which is a material property of the REBCO tape. It is the n -exponent that causes the dependence of the electric field correction factor on magnetic field and temperature. However, as the expression in (7) has the form of an inverse power function, the dependence is usually weak and within given experimental limits the K_e can be often considered as constant, with a reasonable accuracy.

Fig. 4 shows the electric field correction factor K_e computed for the square-shaped samples at 70 K and different magnetic fields for all three tapes, qualitatively very similar situation is observed at the remaining temperatures as well. As can be seen, the factor K_e in general decreases with increasing magnetic field, which is an obvious consequence of the n -exponent decrease. From the three investigated tapes the K_e stays the most constant for the Superpower tape, varies somewhat more in case of the Superox tape and the least constant is for the Sunam tape. The non-smooth shape of the curves is caused by the fluctuation of n -exponent deduced from transport I-V measurements. Considering the K_e determined in the full explored range of $B = 0.25 \text{ T} - 2 \text{ T}$ and $T = 65 \text{ K} - 77 \text{ K}$, the overall spread of the values (i.e. $\max(K_e)/\min(K_e) - 1$) is approximately 15% for the Superox tape, 19% for Sunam and 16% for Superpower.

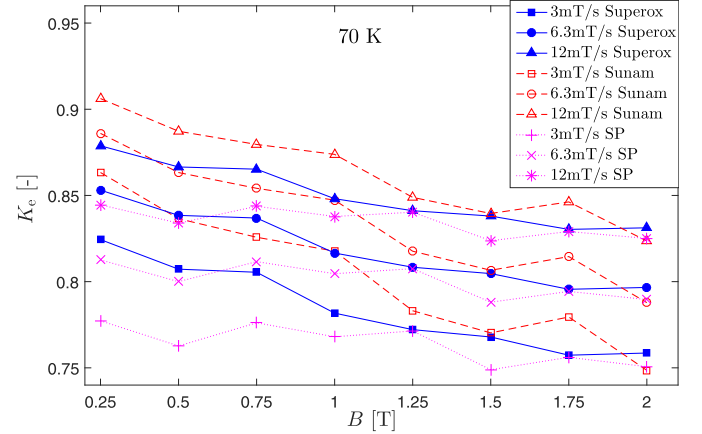


Fig. 4. Electric field correction factor K_e at 70 K for all three tapes (square-shaped samples). The lines are guides to the eye.

The magnetic field dependence of the theoretically derived correction factor K_e can be compared with the experimental data of Δm and J_c determined in independent magnetization and transport measurements. In the Fig. 5, the ratio $\Delta m/J_c$, which the empirical scaling factor is based on, is plotted in dependence on the applied magnetic field B together with the electric field correction factor K_e for the square-shaped samples at 70 K. Similar picture is observed at other temperatures as well. To display both quantities in one graph, the $\Delta m/J_c$ values are scaled with a suitable factor N for each sample (N_1 for Superox, N_2 – Sunam, N_3 – Superpower). Value of N is given as the geometrical constant C_g multiplied by a small numerical factor $\alpha \sim 1$, i.e. $N_1 = \alpha_1 C_g$ (Superox) and similarly for Sunam and Superpower, with $\alpha_1 = 0.901$, $\alpha_2 = 1.115$ and $\alpha_3 = 0.924$. The trends observed in Fig. 5 suggest that the change in n -exponent having as a consequence the variation of electric field correction factor K_e is the most significant cause for the observed reduction of scaling factor with magnetic field.

The theoretical counterpart of the empirical scaling factor F_{77} can be defined as $\varphi_{77} = C_g/K_e(0.25 \text{ T}, 77 \text{ K})$, considering the K_e based on the n -exponent determined at the experimentally convenient $T = 77 \text{ K}$, $B = 0.25 \text{ T}$, $s = 6.3 \text{ mT/s}$. Comparison of the empirical and theoretical scaling factors for the *square-shaped* samples shows that the ratio φ_{77}/F_{77} is 1.128 for Superox, 0.902 for Sunam and 1.110 for Superpower tape. In the case of the *rectangular* samples we have only the magnetization data at 70 K, 6.3 mT/s and the comparison of the $\varphi_{70} = \varphi(0.25 \text{ T}, 70 \text{ K})$ with the empirical scaling factor $F_{70} = F(70 \text{ K})$

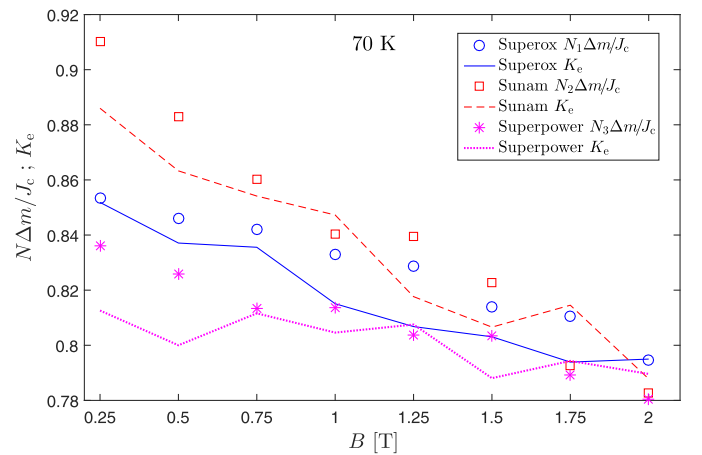


Fig. 5. Electric field correction factor K_e (lines) and experimental values of $\Delta m/J_c$ (symbols) at 70 K for all three tapes (square-shaped samples). The $\Delta m/J_c$ values are scaled with factors $N_1 = 2.7510^{14} \text{ m}^{-4}$ (Superox), $N_2 = 2.810^{14} \text{ m}^{-4}$ (Sunam) and $N_3 = 1.9510^{14} \text{ m}^{-4}$ (Superpower) in order to display in one plot with K_e .

yields $\varphi_{70}/F_{70} = 0.872$ for Superox, 1.033 for Sunam and 0.975 for the Superpower tape. Values of the scaling factors are presented in the Table 1.

In general, the scaling factors estimated theoretically agree with the empirical ones within approximately 10%, which supports the relevance of the simple analytical considerations outlined in this section. These considerations unveil the theoretical basis of the proposed empirical scaling and its relationship with the well known Eq. (2), commonly used to derive the critical current density from the measured magnetic moment. As it is visible from Eqs. (7) and (8), the theoretically expected variation of the scaling factor with field and temperature follows from the variation of the electric field correction factor K_e . The dependence on B and T enters through the power law exponent $n(B, T)$ in the form of inverse power function. This functional form considerably reduces the total impact of n -exponent variation. It is thus often possible to consider the scaling factor as constant over certain range of B and T with a good accuracy, although absolutely strictly speaking the scaling factor is different whenever there is a variation in $n(B, T)$. The closer to each other are the electric field levels at the transport (E_c) and at the magnetization ($E_{i, \text{mag}}$) measurements, the less pronounced is the impact of the $n(B, T)$ variation. Electric field induced in the sample can be to a certain limited extent adjusted by selection of the sample dimensions and sweep rate in the magnetization experiment.

The analytical expressions also enable to estimate the variation between scaling factors at different experimental conditions. Let's consider in general two experimental conditions, "1" and "2":

$$\begin{aligned} 1: B_1, T_1 &\rightarrow n(B_1, T_1) = n_1; K_e(B_1, T_1) = K_{e1} \\ 2: B_2, T_2 &\rightarrow n(B_2, T_2) = n_2; K_e(B_2, T_2) = K_{e2} \end{aligned}$$

The ratio of the scaling factor φ_1 at B_1, T_1 and φ_2 at B_2, T_2 is straightforwardly expressed as:

$$\frac{\varphi_2}{\varphi_1} = \frac{K_{e1}}{K_{e2}} = \left(\frac{lws}{2(l+w)E_c} \right)^{1/n_1 - 1/n_2} = \varepsilon^{(n_2 - n_1)/(n_1 n_2)}. \quad (9)$$

Here we assume the same sweep rate s employed at both conditions and electric field ratio $\varepsilon = E_{i, \text{mag}}/E_c$ is introduced for convenience. The change in scaling factor between 1 and 2, expressed as the ratio φ_2/φ_1 , thus depends on the sample size (shape) and the other experimental parameters included in ε as well as on the properties of the investigated coated conductor reflected in the power law exponents n_1 and n_2 . An example interesting in practice could be the comparison between $T_1 = 77$ K, $B_1 = 0.25$ T and $T_2 \sim 4.2$ K, $B_2 \sim 2 - 10$ T. One can consider $n_1 \sim 20$ and $n_2 \sim 50$ as typical values of power law exponent for commercial CC's at these conditions, which yields for our case ($\varepsilon \approx 0.032$) the estimate of the scaling factor variation $\varphi_2/\varphi_1 \approx 0.902$. That means approximately 10% error could be expected when the scaling factor from 77 K is used at 4.2 K.

Calculation of transport J_c on the basis of the theoretical relation (6) is also possible, however, it is in practice equivalent to the empirical scaling as at least one transport measurement would be necessary to determine the required n -exponent. Note also that as far as only the critical current I_c is considered, the empirical scaling can be employed in the same way as described in the Section 3 (modifying F to $F' = I_c/\Delta m$) without a need to determine any geometrical dimensions. In contrast the calculation of the theoretical scaling factor always requires the geometrical dimensions of the magnetization sample, which are often difficult to precisely determine. Direct empirical scaling is to our opinion more straightforward and more accurate.

5. Conclusion

The article presents a comparison of experimental $J_c(B)$ dependences determined in magnetization and transport measurements in the temperature range 65 K – 77 K for commercial coated conductors of

three different industrial manufacturers. We have shown that in the explored temperature and field range it is possible to empirically rescale the measured magnetization data Δm to predict the transport J_c using a simply defined numerical factor F , achieving a reasonable accordance. The experimental data were compared at applied magnetic fields high enough to neglect the transport self-field effects and to ensure a full sample penetration with a single direction magnetization currents in the magnetization experiments.

The demonstrated possibility of using a single value of the scaling factor F_{77} to rescale the magnetization data is very interesting from the practical point of view, as it enables to "calibrate" the $\Delta m(B)$ curves on the basis of a single transport measurement performed at an experimentally convenient temperature. The presented basic theoretical analysis shows that calibration of this type is only approximate, however, its overall accuracy can be reasonable and in practice it can be very useful. From the analysis it follows that the extent to which the scaling factor F can be considered constant is governed by the variation of the electric field correction factor K_e with field and temperature. The correction factor K_e is given as the ratio of the typical electric field in the magnetization sample and the transport electric field criterion (1 $\mu\text{V}/\text{cm}$), taken to the power $1/n$, $n(B, T)$ being the exponent of the power-law $E(J)$ relation (see (5)). This means that the closer is the electric field in the sample to the transport criterion and the smaller is the variation of the n -exponent in the considered temperature and magnetic field range, the more constant is the resulting scaling factor.

Acknowledgement

This work was supported by the Slovak Academy of Sciences and the European Union in the framework of the SASPRO programme under Contract No. 1633/03/01, by the VEGA grant agency under Contract No. 2/0097/18 and by implementation of the project: Centre for development and application of advanced diagnostic methods in processing of metallic and non-metallic materials (ITMS: 26220120048) supported by the Research and Development Operational Programme funded by the ERDF (Grant No. 26220120048).

References

- [1] K. Kakimoto, Y. Iijima, T. Saitoh, Fabrication of long-Y123 coated conductors by combination of IBAD and PLD, *Physica C* 392 (2003) 783.
- [2] V. Selvamanickam, Y. Chen, X. Xiong, Y.Y. Xie, J.L. Reeves, X. Zhang, Y. Qiao, K.P. Lenseth, R.M. Schmidt, A. Rar, D.W. Hazelton, K. Tekletsadik, Recent progress in second-generation HTS conductor scale-up at superpower, *IEEE Trans. Appl. Supercond.* 17 (2007) 3231.
- [3] C. Senatore, M. Alessandrini, A. Lucarelli, R. Tediosi, D. Uglietti, Y. Iwasa, Progresses and challenges in the development of high-field solenoidal magnets based on RE123 coated conductors, *Supercond. Sci. Technol.* 27 (2014) 103001.
- [4] A.P. Malozemoff, Second-generation high-temperature superconductor wires for the electric power grid, *Annu. Rev. Mater. Res.* 42 (2012) 373.
- [5] P.V. Gade, C. Barth, C. Bayer, W.H. Fietz, F. Franza, R. Heller, K. Hesch, W. K-P, Conceptual design of a toroidal field coil for a fusion power plant using high temperature superconductors, *IEEE Trans. Appl. Supercond.* 24 (2014) 4202705.
- [6] X. Obradors, T. Puig, Coated conductors for power applications: materials challenges, *Supercond. Sci. Technol.* 27 (2014) 044003.
- [7] L. Rossi, X. Hu, F. Kametani, D. Abrahimov, A. Polyanski, J. Jaroszynski, D.C. Larbalestier, Sample and length-dependent variability of 77 and 4.2K properties in nominally identical RE123 coated conductors, *Supercond. Sci. Technol.* 29 (2016) 054006.
- [8] Q. Jiang, M. Majoros, Z. Hong, A.M. Campbell, T.A. Coombs, Design and AC loss analysis of a superconducting synchronous motor, *Supercond. Sci. Technol.* 19 (2006) 1164.
- [9] A.B. Abrahamsen, N. Mijatovic, E. Seiler, T. Zirngibl, C. Træholt, P.B. Nørgård, N.F. Pedersen, N.H. Andersen, J. Østergård, Superconducting wind turbine generators, *Supercond. Sci. Technol.* 23 (2010) 034019.
- [10] T.M. Qu, et al., Development and testing of a 2.5 kW synchronous generator with a high temperature superconducting stator and permanent magnet rotor, *Supercond. Sci. Technol.* 27 (2014) 044026.
- [11] J. Leclerc, P.J. Masson, Testing of a subscale hts coil for wind turbine generator, *IEEE Trans. Appl. Supercond.* 26 (2016) 5206304.
- [12] H. Moon, Y.C. Kim, H.J. Park, M. Park, I.K. Yu, Development of a MW-class 2G HTS ship propulsion motor, *IEEE Trans. Appl. Supercond.* 26 (2016) 5203805.
- [13] X.W. Song, et al., A full-size high-temperature superconducting coil employed in a wind turbine generator setup, *IEEE Trans. Appl. Supercond.* 27 (2017) 5201105.

- [14] A. Xu, L. Delgado, N. Khatri, Y. Liu, V. Selvamanickam, D. Abrahimov, J. Jaroszynski, F. Kametani, D.C. Larbalestier, Strongly enhanced vortex pinning from 4 to 77 K in magnetic fields up to 31 T in 15 mol.% Zr-added (Gd, Y)-Ba-Cu-O superconducting tapes, *Appl. Phys. Lett. Mater.* 2 (2014) 046111.
- [15] L. Frolek, J. Souc, Measurement of current-voltage curves of superconducting tapes by means of quasi trapezoidal current impulses, *IEEE Trans. Appl. Supercond.* 19 (2009) 3581.
- [16] F. Roy, B. Dutoit, F. Sirois, Evaluation of the applicability of phenomenological HTS models for numerical analysis of quenches in coated conductors: simulations vs. experiments, *IEEE Trans. Appl. Supercond.* 21 (2011) 1190.
- [17] K.W. See, X. Xu, J. Horvat, C.D. Cook, S.X. Dou, Transport critical current of MgB₂ wires: pulsed current of varying rate compared to direct current method, *Supercond. Sci. Technol.* 24 (2011) 105009.
- [18] M. Ciszek, S. Trojanowski, Low noise measurement system for determination of the critical currents in superconducting tapes by a pulse method, *Rev. Sci. Instrum.* 82 (2011) 114701.
- [19] C. Senatore, C. Barth, M. Bonura, M. Kulich, G. Mondonico, Field and temperature scaling of the critical current density in commercial REBCO coated conductors, *Supercond. Sci. Technol.* 29 (2016) 014002.
- [20] X. Xiong, S. Kim, K. Zdun, S. Sambandam, A. Rar, K.P. Lenseth, V. Selvamanickam, Progress in high throughput processing of long-length, high quality, and low cost IBAD MgO buffer tapes at Superpower, *IEEE Trans. Appl. Supercond.* 19 (2009) 3319.
- [21] S.S. Oh, et al., Development of long-length SmBCO coated conductors using a batch-type reactive co-evaporation method, *Supercond. Sci. Technol.* 21 (2008) 034003.
- [22] S. Lee, V. Petrykin, A. Molodyk, S. Samoilenkov, A. Kaul, A. Vavilov, V. Vysotsky, S. Fetisov, Development and production of second generation high T_c superconducting tapes at Superox and first tests of model cables, *Supercond. Sci. Technol.* 27 (2014) 044022.
- [23] C.P. Bean, Magnetization of hard superconductors, *Phys. Rev. Lett.* 8 (1962) 250. Bean C P, Magnetization of high-field superconductors, *Rev. Mod. Phys.* 36 (1964) 31.
- [24] O. Polat, J.W. Sinclair, Y.L. Zuev, J.R. Thompson, D.K. Christen, S.W. Cook, D. Kumar, Y. Chen, V. Selvamanickam, Thickness dependence of magnetic relaxation and E-J characteristics in superconducting (Gd-Y)-Ba-Cu-O films with strong vortex pinning, *Phys. Rev. B* 84 (2011) 024519.
- [25] I.A. Golovchanskiy, A.V. Pan, O.V. Shcherbakova, S.A. Fedoseev, Rectifying differences in transport, dynamic, and quasi-equilibrium measurements of critical current density, *J. Appl. Phys.* 114 (2013) 163910.
- [26] E.H. Brandt, Determination of currents in flat superconductors, *Phys. Rev. B* 46 (1992) 8628.
- [27] E.H. Brandt, M. Indenbom, Type-II-superconductor strip with current in a perpendicular magnetic field, *Phys. Rev. B* 48 (1993) 12893.
- [28] J.R. Clem, A. Sanchez, Hysteretic ac losses and susceptibility of thin superconducting disks, *Phys. Rev. B* 50 (1994) 9355.
- [29] F. Gömöry, R. Tebano, A. Sanchez, E. Pardo, C. Navau, I. Husek, F. Strycek, P. Kovac, Current profiles and ac losses of a superconducting strip with an elliptic cross-section in a perpendicular magnetic field, *Supercond. Sci. Technol.* 15 (2002) 1311.
- [30] A.M. Campbell, J.E. Evetts, Flux vortices and transport currents in type II superconductors, *Adv. Phys.* 21 (1972) 199.
- [31] C. D-X, R.B. Goldfarb, Kim model for magnetization of type-II superconductors, *J. Appl. Phys.* 66 (1989) 2489.
- [32] M. Zehetmayer, Simulation of the current dynamics in superconductors: application to magnetometry measurements, *Phys. Rev. B* 80 (2009) 104512.